Extended Abstract Submitted to the 19th AIAA/CEAS Aeroacoustics Conference, Berlin, Germany SAND2012-9413C

Validation of an FSI Modeling Framework for Internal Captive Carriage Applications

Srinivasan Arunajatesan[1], Mike Ross[2], Tyler Jordan Garrett[3]
Sandia National Laboratories, Albuquerque, NM.

A fluid-structure interaction framework has been developed at Sandia for the simulations of stores in captive carriage situations. The framework couples aerodynamic loads computed using a Computational Fluid Dynamics (CFD) Solver, SIGMA CFD with a Computational Structural Dynamics (CSD) solver, Sierra/SD or Salinas, to predict the response of the store to the aerodynamic loads. Loose (boundary conditions only), one-way (small deflections) coupling is used in the framework. The consistency and accuracy of the load transfers, along with convergence behavior of the coupled framework predictions were demonstrated in an earlier paper. In this work, we are focused on validation of the framework against carefully conducted experiments that simultaneously measure cavity pressures and store response.

I. Introduction

The large fluctuating surface pressure loads observed in aircraft weapons bay surfaces represent a serious concern for future military aircraft and stores carried within them. The weapons bay flowfield is very strongly affected by many characteristics such as the flight velocity, the bay geometric features, the presence of stores in the bay, the upstream boundary layer etc[1-3]. Over the past few decades numerous studies have been aimed at developing a fundamental understanding of the physical mechanisms which drive these fluctuating pressures[4-6], including some successful computational modeling efforts[7,8]. Our interest in these flow fields concerns the response of the stores when subjected to this harsh environment.

If the loads are large enough and contain energy in the right frequency ranges, it is possible that the store and its components can be dramatically affected. This effect can be an important consideration that must be included in the store design and qualification process.

In an earlier paper[9], we presented a fluid-structure interaction (FSI) modeling framework that couples a fluid dynamics solver, SIGMA CFD, with a structural dynamics solver (Sierra/SD or Salinas) to model the effects of the unsteady loads on the store structure and its components. This framework is used in the present work also. As was described in detail in Ref. [9], the coupling between the two codes is done through boundary conditions only – the two equation systems are still solved separately. In addition to this, the deflections computed by the structural dynamics solver are not passed back to the CFD code – the CFD code assumes rigid structures in its computations. These assumptions and their implications were discussed in detail, along with accuracy, consistency and convergence issues. Here, we are interested in the validation of the predictions made using this framework for a model problem. Careful experiments have been designed and are being carried out to provide data on both, the cavity flow field as well as the store response, to support this effort.

This paper is organized as follows. Section II provides a brief description of the FSI framework. Validation of the aerodynamic load predictions (without store responses) is discussed in section III. Section IV presents a brief discussion of the experimental configuration and the structural model development along with results from the application of the framework to the problems of interest and Section V discusses the contents of the final paper.

II. Sandia's FSI Modeling Framework

As mentioned above, the details of the FSI framework were described in detail in Ref. [9] – only a brief review is presented here. In this approach, the CFD code provides unsteady pressures as boundary loads to the CSD solver.

[1] Staff Tech, Sandia National Laboratories, Senior Member AIAA.
[2] Staff Tech, Sandia National Laboratories, Senior Member AIAA.
[3] Staff Tech, Sandia National Laboratories, Member AIAA.

The deflections computed by the CSD solver are, however, not felt by the CFD solver. The CFD solver assumes a rigid and stationary structure when computing the flow around it.

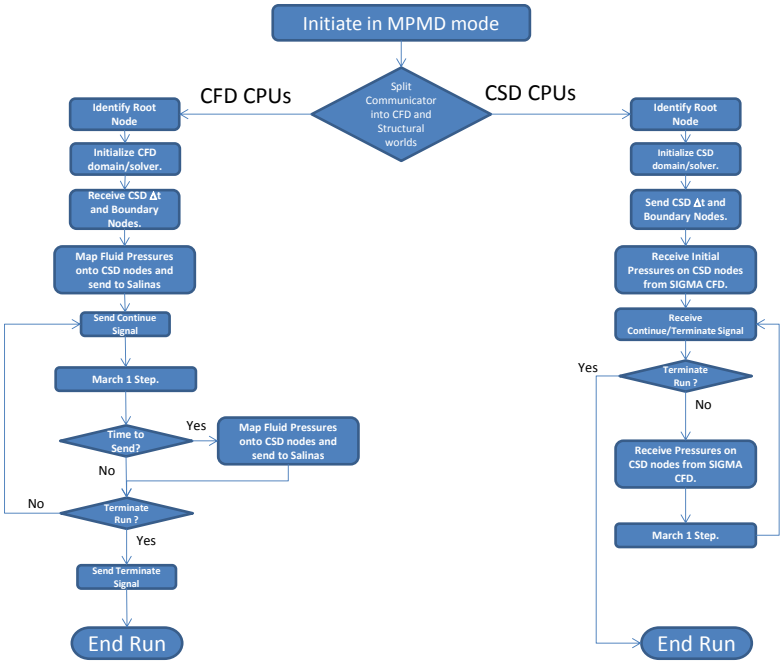

Figure 1. Flow chart of the FSI coupled simulation procedure.

To carry out FSI calculations, the two codes are executed in multiple program multiple data (MPMD) mode using the "mpiexec" command. In this manner, the two codes can be used either as standalone executables or in coupled mode. The overall flow chart describing the steps in the coupled calculation is shown in Figure 1. When initiated, the two codes share a common communication world (handle) that is used to communicate between the two codes. This communicator is split to separate out the CFD and CSD worlds – the two solvers perform all independent operations using these split communicators. After initializing their respective domains, the structural solver sends the boundary nodes on which the pressures are required and the frequency (time intervals) at which this is required for the structural solves. The CFD code then creates and stores a map of the CSD nodes on the surface – this map identifies the CFD nodes (and their interpolation weights) surrounding each CSD node. This map is then used to project the initial CFD pressures on to the CSD node and these pressures are then sent to the CSD code to use as a pre-load condition.

In our earlier work[9], we compared two different interpolation methods for transferring the fluid pressures onto the structural mesh. In the first method, the pressure from the nearest CFD node is used at the CSD node. In the second method, the CFD face on which the CSD node falls is determined and linear basis functions are used to interpolate the pressures to the CSD node from the CFD nodes of that face. It was demonstrated that the difference in the overall forces using the two methods was less than about 3%. Hence, the nearest node approach is used in this work.

The communications between the two codes is handled using a simple API that handles all communications between the codes and the communicator management. Communications between the CFD and CSD codes are carried out through the root nodes in each world. This entails global reduction/gather/scatter operations on each side, but runs with large disparities in processor counts between the CSD (64 CPUs) and CFD (8192 CPUs) models do not show any prohibitive additional overhead due to this mode of operation.

III. Validation of Aerodynamic Load Predictions

The CFD code used in the present work is SIGMA CFD. The first step in making FSI predictions of store and component response is to validate the aerodynamic load predictions. In order to develop confidence that the pressure loads are accurately predicted for the captive carry scenarios of interest, we have carried out simulations of

rectangular cavity configurations that have been published in the literature. Comparisons of the wall pressure Power Spectral Densities (PSDs) and velocity field data (where available) are carried out to develop confidence in the CFD predictions.

The predictions themselves are carried out using a formally second order accurate scheme. The flux reconstruction for the inviscid fluxes is fifth-order accurate[10] and uses the Roe scheme; the viscous terms are evaluated using a second order central difference scheme. The turbulence model used is a hybrid RANS-LES model based on the $k-\varepsilon$ turbulence model developed for cavity flow predictions[11]. A sponge region[12] has also been implemented in order to prevent spurious reflections from far field boundaries for aero-acoustics problems. At the viscous walls (upstream of the cavity and the cavity walls) a wall layer model that accounts for non-equilibrium effects (pressure gradient)[13] is used. An implicit LU-SGS scheme with 3 Newton iterations at each time step is used for time advancement.

A. Validation against WICS Cavity Database

Validation of the code for the simulations of cavity flows has been carried out using the WICS cavity flow database[14]. Results from simulations at Mach 0.6 and Mach 0.95 flow over a length to depth ratio L/D=4.5 and width to depth ratio W/D=2 cavity have been compared to measured values. In this database, only wall pressure spectra measurements are available. Results from the Mach 0.6 flow is show in Figure 2(a) - a comparison of the wall pressure spectra for one of the aft wall sensors against the WICS cavity flow data is shown. Results from the Mach 0.95 flow at the same sensor location is shown in Figure 2(b). These results are representative of the results obtained at all the sensor locations. It is clear from these plots that the predictions of the wall pressures are in good agreement with the measured values. The dominant modes (Rossiter modes 2 and 3, in these cases) are accurately captured by the simulations. The overall sound pressure levels (OASPL) along the cavity floor for these two cases is shown in Figure 2 (c) and (d). It is clear from these again, that the predictions are in good agreement with the measured values over all the locations.

These predictions of fluctuating wall pressure levels and spectra provide some confidence that the loads transferred to the structural solver in the FSI framework are accurate enough to make reliable predictions of the component response. However, the WICS cavity database does not provide flow field (velocities and turbulence levels) information and it is important to ensure that the predictions of these are in good agreement with measured values as well. In addition, a store is likely to be positioned in the middle of the cavity and accurate predictions of the velocity field and turbulent stresses in the middle of the cavity is likely to provide greater confidence in the pressure field in that region. In order to ascertain this, comparisons of the mean and turbulent velocity field measured on similar flow configurations and presented in the open literature have also been carried out.

B. Validation of the Mean and Turbulent flow field

Simulations of the flow configuration studied by Murray and Ukeiley[15] have been carried out to validate the flow field predictions. The flow configuration consists of a Mach 0.58 flow over a L/D=6 cavity (L=48mm, D=8mm) that spanned the 2" test section wind tunnel. The wall of the test section opposite was treated to ensure no acoustic reflections were present. Wall pressure measurements were made on the mid-span plane of the cavity along with PIV measurements on the same plane. The PIV measurements provide values of the mean and rms velocities (turbulent stresses) on the mid-span plane.

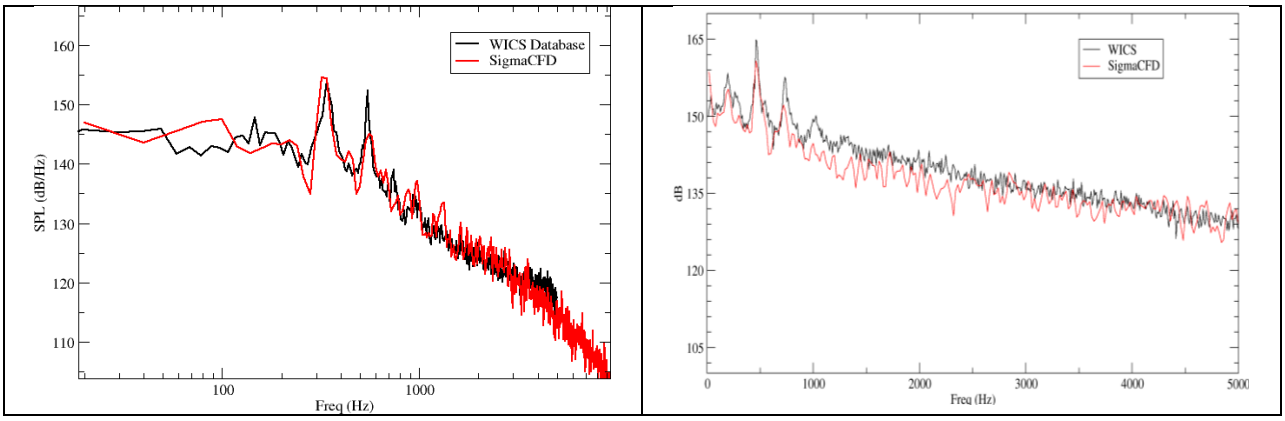

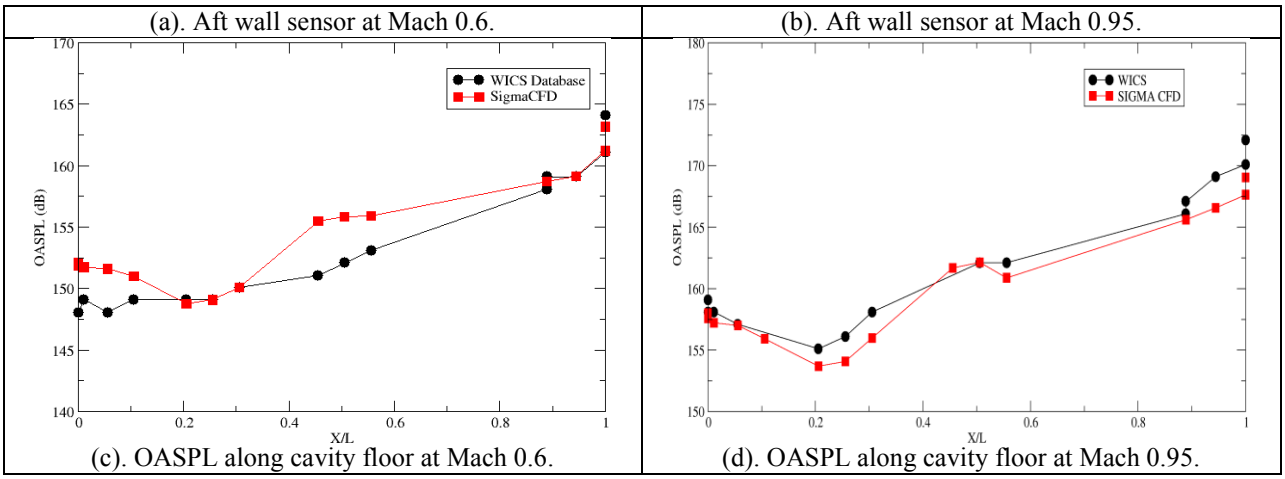

Figure 2. Comparison of the computed aft wall pressure spectrum (for sensor K18 in the WICS database) and overall sound pressure levels on the cavity floor with the corresponding measured values from the WICS database.

Comparisons of the wall pressure spectrum at the mid-point of the aft wall and overall sound pressure levels along the cavity floor are shown in Figure 3. Here again, good overall agreement is seen for the spectrum. The dominant modes are correctly captured with a 4% difference in frequencies for mode 3. The OASPL levels are again predicted within 1-2 dB of measured values for the entire region, giving us some confidence that the simulation is capturing the important dynamics of the flow field correctly.

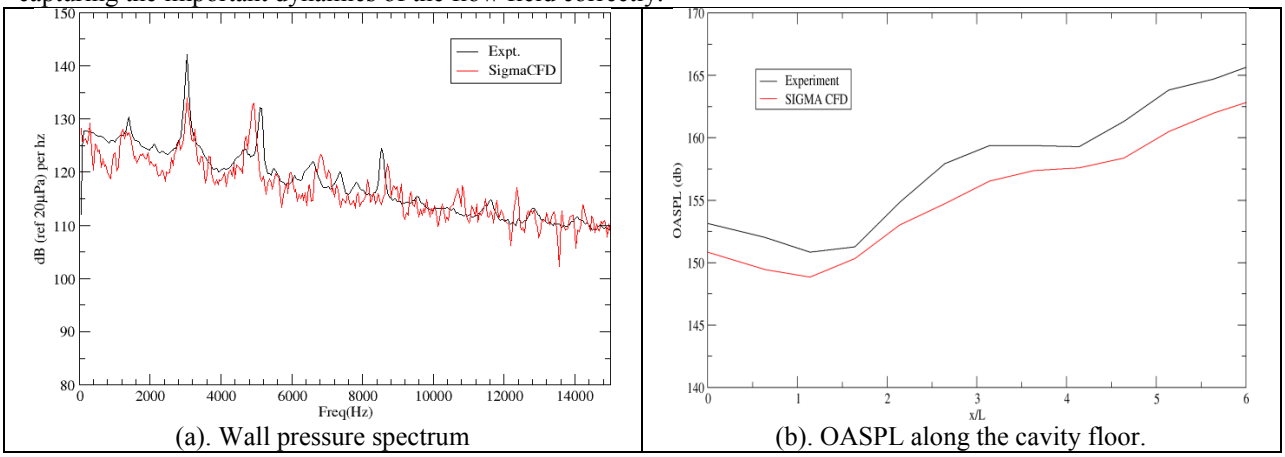

Figure 3. Comparison of the predicted wall pressure data - spectrum at the aft wall and OASPL along the cavity floor with corresponding measured values for the Murray and Ukeiley cavity flow case[15].

Comparisons of the mean streamwise velocity and the turbulent stresses with the measured values from the PIV data are presented in Figure 4 (a) and (b). The mean velocity profile is clearly in very good agreement with the measure profile. The turbulent stresses are also in reasonable agreement with the measured values – both the magnitude and the locations of the peak are predicted in reasonable agreement with the measured values.

These comparisons provide a high degree of confidence that the computational pressure loads being transferred to the structural solver in the FSI framework are accurately modeled and that these provide an accurate representation of the dynamics of the flow field. This is a crucial step in ensuring that the coupled predictions are accurate.

Next, we present a discussion of the FSI model configuration and the structural model development.

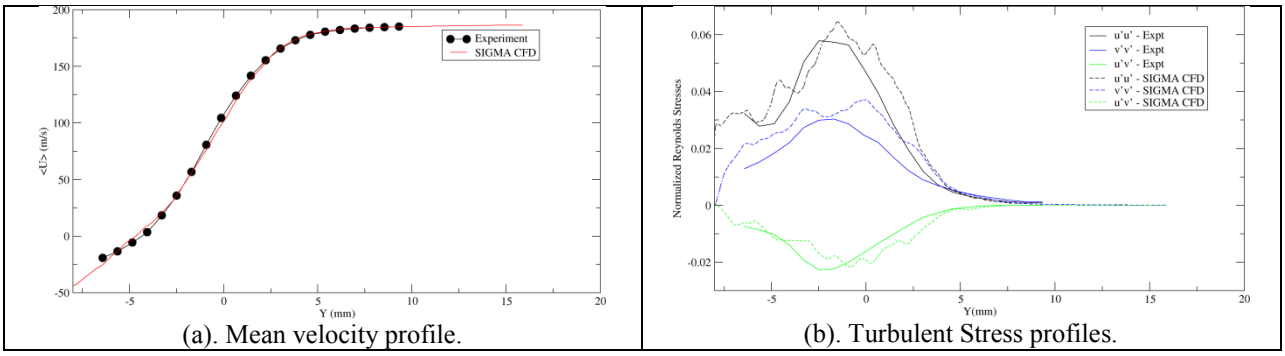

(a). Mean velocity profile. (b). Turbulent Stress profiles.

Figure 4. Comparisons of the mean streamwise velocity profile and turbulent stress profiles at a station 37mm downstream of the leading edge of the cavity with measured profiles.

IV. The FSI Validation Configuration

A. Experimental Setup

As mentioned earlier, the experiments for the FSI validation are being conducted at Sandia[16]. Experiments are conducted in the blowdown-to-atmosphere Tri-sonic Wind Tunnel. The facility uses air as the test gas and has a 305 × 305 mm2 test section that is enclosed in a pressurized plenum. Tests are conducted at a freestream Mach number of 0.8, over a stagnation pressure range from 110-250 kPa, which results in a unit Reynolds number range of 14 × 10^6 m^{-1} through 32 × 10^6 m^{-1}. During a run, the stagnation temperature is held constant at 321 ± 2K, and the test section wall temperature remains close to ambient at T_w = 307 ± 3K.

For the FSI validation experiments, an insert is used that fits into the top wall of the test section. As shown in Figure 5, the insert contains a rectangular cavity cutout having a streamwise length *l*, spanwise width *w*, and wall-normal depth *h* of 127 mm, 127 mm, and 38 mm, respectively. Note that the cavity is a modification of a similar design used in Ref. [17]. To provide the aeroacoustic loading data, fast-response pressure sensors (Kulite XCQ-062-30A or similar) will be installed along the cavity floor and back wall.

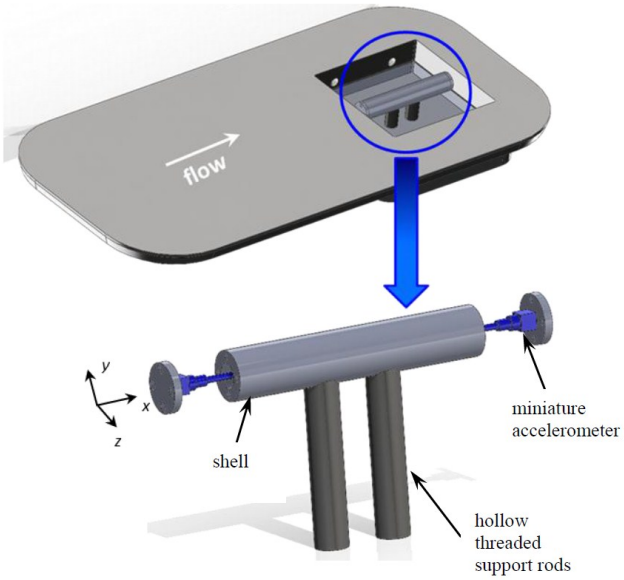

Figure 5. Wind tunnel floor insert containing the rectangular cavity and an assembly view of the cylindrical store model.

In the current work, simplified store geometry is used. As shown in Figure 5, the 108.0 mm-long cylindrical store consists of a hollow, thick aluminum shell having an outer diameter of 38.1 mm and an inner diameter of 9.5 mm. Flanges of thickness 3.2 mm bolt to each end of the shell and serve as attachment points for miniature accelerometers. The store is mounted to the cavity floor with two hollow threaded (thread pitch of UNC ½-13) rods that have an inner diameter of 8.7 mm. The accelerometer leads exit the test section through the hollow support rods. The rods are threaded into the cylindrical body and secured with a thread locking compound (Loctite 262). The rods

attach to the cavity floor with nuts and are spaced 25.4 mm apart. Note that the flow-side nuts sit in counter-bored holes to minimize flow disturbances. The wind tunnel tests will are conducted with the top of the store flush with the wind tunnel floor.

B. Structural Model Development for FSI Calculations

The main effort of this work is to validate the FSI methodology. It would also be an added benefit if it were possible to use this study to quantify any error associated with the FSI methodology. Therefore, it is imperative to have a validated structural model where the error introduced by the structure model is known. This section describes the structural model and details the verification and validation that will be performed on the structural portion of the model.

The structural model was developed in Cubit from a SolidWorks model. The finite element model is discretized with 10 node tetrahedral elements. The material parameters used in the model are defined in Table 1. The casing of the structure is aluminum. Because, the specimen is relatively small, the mass and the stiffness of the accelerometers (one at each end) had to be accounted for in the model as well. These were modeled as cubes with a dimension of 0.25 (inches) that were made of aluminum. In addition, the steel connector of the accelerometer to the cooper wire was modeled in the finite model. Finally, a portion of the copper wire was modeled and the density of the copper wire adjusted to match the measured weight of the specimen. The remainder of this section is a work in progress, but should follow the basic path described below.

Table 1. Structural Model Material Parameters

Material	Density (*lb/in*^{3})	Poisson Ratio	Young's Modulus (*psi*)
Aluminum	0.0975	0.33	$10x10^6$
Steel	0.29	0.29	$29x10^6$
Copper	0.32	0.34	$18x10^6$

The first step in the modeling process is solution verification in the form of a mesh refinement study. Three different mesh densities were used in a modal analysis with the based fixed for the mesh refinement study. Richardson extrapolation is used to determine the converged eigensolution. The first three natural frequencies were converged within 2% and the next seven were converged with 5%. The tenth mode is above 6 KHz, which is deemed appropriate for the study.

After the solution verification, calibration of the model will begin using the fixed base modes of the structure. The fixed base modes of the structure are found using the wind tunnel insert, where the text specimen columns are fixed to the floor of the wind tunnel insert. The difficult aspect of modeling the structure is determining the location of the fixed base. The columns of the test specimen are fixed to the floor of the insert with nut/washer combination on each side of the floor. A locking compound was used on the nuts to provide the best fixed base representation. The distance from the base of the cylinder of the tube to the floor is modified in the structural model for calibration of the modes of the system.

Finally, model validation is accomplished with use of a shaker table test. The difficult aspect of the shaker table is the fact that the fixture has an interaction with the test specimen. Therefore, a portion of the fixture is also modeled. The portion that is modeled is the plate that is attached to the shaker through four studs and is the base where the columns of the test specimen are attached. Once again, the test specimen is fixed to the plate by a nut/washer combination on each side of the plate. The difference noted in the calibration exercise will be used for determining the distance of the columns. The input is applied to the plate at the four corners where the studs from the shaker attach to the plate. This work is still in progress. It is assumed that there will be relative good agreement and that any differences noted can be used to quantify the error in the structural model. This error can be noted in uncertainties that will be propagated to assess any uncertainties in the FSI methodology.

C. FSI Analysis

The computational mesh for the CFD analysis has been generated – the geometry modeled is shown in Figure 6. The mesh generation exploits the use of the wall model and employs a spacing on the walls that is expected to lie roughly around a y^+=50-75. Once the structural model has been validated the calculations can be carried out. The validation is expected to be complete by November of 2012 and the analysis, by Jan 2013.

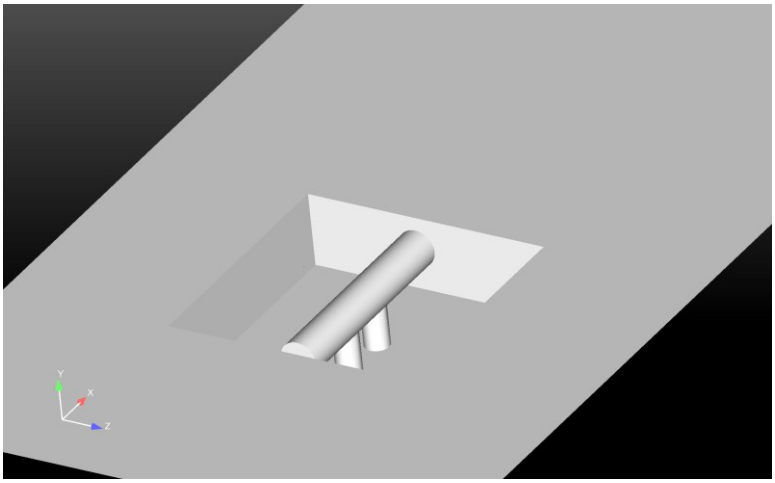

Figure 6. Computational configuration being analyzed in this work for validation.

V. Contents of the Final Paper

The Detailed analysis of the results from the calculations carried out using the above framework will be presented in the final paper. Resolution studies will be carried out by systematically refining the CFD and CSD meshes to determine the consistency and mesh convergence of the predicted responses. Detailed discussions of these will be included in the final paper. In addition to this, the response of the store will be analyzed and correlations with wall pressure histories are expected to be identified. These will be presented and discussed in the final paper.

VI. Acknowledgement

Sandia National Laboratories is a multi-program laboratory managed and operated by Sandia Corporation, a wholly owned subsidiary of Lockheed Martin Corporation, for the U.S. Department of Energy's National Nuclear Security Administration under contract DE-AC04-94AL85000.

VII. References

1. Krishnamurty, K., "Acoustic Radiation from Two-Dimensional Rectangular Cutouts in Aerodynamic Surfaces," NACA, Technical Note 3487, 1955.
2. Rossiter, J., Aeronautical research council reports and memoranda No.3438, 1964
3. Roshko, A., "Some Measurements of Flow in a Rectangular Cutout," NACA, Technical Note 3488, 1955
4. Zhuang, N., Alvi, F.S., Alkislar, M.B., Shih, C., Sahoo, D. and Annaswamy, A.M., "Aeroacoustic Properties of Supersonic Cavity Flows and Their Control", AIAA-2003-3101.
5. Murray, N.E., and Ukeiley, L.S., "Flow Field Dynamics in Open Cavity Flows", AIAA-2006-2428.
6. 2006 aeroacoustics paper
7. Nichols, R.H., "Comparison of Hybrid Turbulence Models for a Circular Cylinder and a Cavity", AIAA Journal, Vol. 44, No. 6, 2006.
8. Arunajatesan, S., Kannepalli, C., Sinha, N., Sheehan, M., Alvi, F. Shumway, G. and Ukeiley, L.S., "Suppression of Cavity Loads Using Leading Edge Blowing", AIAA Journal, Vol. 47, No. 5, 2009.
9. Arunajatesan, S., Bhardwaj, M., Riley, W.C., Ross, M., "One-Way Coupled Fluid Structure Simulations of Stores in Weapons Bays", Accepted for presentation at the 51st AIAA Aerospace Sciences Meeting, Grapevine, Tx.
10. Rai, M.M, "Navier-Stokes Simulations of Blade-Vortex Interaction Using High-Order Accurate Upwind Schemes", AIAA-87-0543.
11. Arunajatesan, S. and Sinha, N., "Hybrid RANS-LES Modeling for Cavity Aeroacoustics Predictions," International Journal of Aeroacoustics, Vol. 2, No. 1, pp 65-91, 2003.
12. Rowley, C.W., Colonius, T., Basu, A.J., "On self-sustained oscillations in two-dimensional compressible flow over rectangular cavities", Journal of Fluid Mechanics, vol. 455, pp. 315-346, 2002.
13. Duprat, C., Balarac, G., Metais, O., Congedo, P.M., Brugiere, O., "A Wall-Layer Model for Large Eddy Simulations of Turbulent Flows with/out Pressure Gradient", Physics of Fluids, 23, 015101, 2011.
14. Dix, R. E., and Bauer, R. C., "Experimental and Theoretical Study of Cavity Acoustics," Arnold Engineering Development Center, Rept. AEDCTR-99-4 (AD-A384010), Arnold AFB, TN, May 2000.
15. Murray, N. and Ukeiley, L.S., "Flow field dynamics in open cavity flows", AIAA-2006-2428, presented at the 12th AIAA/CEAS aeroacoustics conference, Cambridge, MA, 2006.

16. Wagner, J.L., Beresh, S.J., Henfling, J.F., Spillers, R.W., Blecke, J., "Simultaneous Vibration and Acoustic Measurements of a Store in a Compressible Open Cavity Flow", Accepted for publication at 51st AIAA Aerospaces Sciences Meeting, Grapevine, TX, 2013.
17. Beresh S. J., Wagner J. L., and Pruett, B. O., "Particle Image Velocimetry of a Three-Dimensional Supersonic Cavity Flow," AIAA Paper 2012-030.
18. Reese, G., Bhardwaj, M., and Walsh, T., "Salinas- Theory Manual," Technical Report SAND2009-0748, Sandia National Laboratories, Albuquerque, NM, 2009.
19. Bhardwaj, M., Pierson, K., Reese, G., Wash, T., Day, D., Alvin, K., Peery, J., Farhar, C., Lesoinne, M., "Salinas: A Scalable Software for High-Performance Structural and Solid Mechanics Simulations", Pre-print submitted to the 2002 Gordon Bell Award, Nov. 2002.
20. Sankaran, V. and Menon, S., "LES of Scalar Mixing in Supersonic Shear Layers," Proceedings of the Combustion Institute, Vol. 30, pp. 2835-2842, 2004
21. Genin, F. and Menon, S., "Studies of Shock/Turbulent Shear Layer Interaction Using Large-Eddy Simulation," Computer and Fluids, Vol. 39, pp. 800-819, 2010.
22. Genin, F. and Menon, S., "Dynamics of Sonic Jet Injection into Supersonic Crossflow," Journal of Turbulence, Vol. 11, Art. No. N 4., 2010.
23. Molvik, G.A., "A Computational Model for the Prediction of Hypersonic Reacting Flows", Ph.D Thesis, Pennsylvania State University, 1989.
24. Chen RF and Wang ZJ, "Fast, Block Lower-Upper Symmetric Gauss Seidel Scheme for Arbitrary Grids", AIAA Journal, vol. 38, no. 12, 2000.
25. Ducros, F., Laporte, F., Souleres, T., Guinot, V., Moinat, P., Caruelle, B., "High-Order Fluxes for Conservative Skew-Symmetric-like Schemes in Structured Meshes: Application to Compressible Flows", Journal of Computational Physics, 161, 2000.
26. Papp, J.L., and Dash, S.M., "Turbulence Model Unification and Assessment for High-Speed Aeropropulsive Flows", AIAA-2001-0880.
27. Wilcox, D. C., Turbulence Modeling for CFD, DCW Industries, 2nd ed., 1998
28. Menter, F.R., "Two-Equation Eddy-Viscosity Turbulence Models for Engineering Applications", AIAA Journal, Vol. 32, No. 8, 1994.
29. Strelets, M., "Detached Eddy Simulation of Massively Separated Flows", AIAA-2001-0879.
30.